PHYSICAL REVIEW VOLUME 180, NUMBER 1 5 APRIL 1969

# Bremsstrahlung and Recombination Radiation of Neutral and Ionized Nitrogen*

J. C. Morris, R. U. Krey, and R. L. Garrison
*Aerophysics Laboratories, Space Systems Division, Avco Corporation, Wilimington, Massachusetts* 01887
(Received 14 October 1968)

Continuum radiation measurements are presented for nitrogen over a spectral range from 975 to 37 000 Å for temperatures ranging from 9000 to 13 500°K and 1- and 2- atm pressure. The measurements were made using a plasma produced in a dc mechanically constricted arc generator. The data is separated by a temperature-dependence curve fit into the contributions from positive-ion and neutral-atom radiation. The $N^+$ radiation is compared to an analytical calculation based on the Burgess and Seaton quantum-defect method for the free bound and on the Gauntfactors of Karzas and Latter for the free-free processes. The remaining radiation in the visible and infrared is ascribed to the neutral atom. This data is analyzed to derive the $N^-$ species responsible for the recombination radiation and to extract its ionization energy from the position of observed absorption edges. A value for the ($N^-$ $^1D$) negative-ion cross section is obtained. Extraction of the neutral atom $Z^2g$ factor for the Bremsstrahlung process was made from the continuum data in the infrared. Comparison is also made to other experimental data.

## INTRODUCTION

The recombination and bremsstrahlung continuum radiation is one of the dominant spectral features of high-temperature high-density plasmas. As a laboratory tool it has been used as a means of temperature[1] and electron number density[2] measurements and as a means for studying the lowering of the ionization energy.[3] In addition to this the continuum is one of the most important modes of radiation energy transfer in stellar atmospheres and in laboratory plasmas such as electric arcs and shocks in shock tubes. Recently it has become of significant interest to that part of the engineering community concerned with heating of high-velocity re-entry space vehicles. Because of this scientific and engineering interest a number of analytical treatments have been forwarded, attempting to predict the magnitude and spectral distribution of the continuum. These predictions however for gases other than hydrogen disagree with each other in some spectral regions by a considerable amount. There have been few experimental studies directed specifically toward gathering data to shed light on the validity of the various predictions available. Of the measurements that do exist many lack spectral purity, i.e., suffer from interference from radiating mechanisms other than the continuum, while others cover wavelength ranges too small to be of significant use for comparison purposes.

The present paper reports the attempts by the authors to overcome some of these difficulties for the case of nitrogen. Nitrogen has been chosen because of its engineering and scientific interest. It constitutes the greatest abundance of our own atmosphere and is responsible for the bulk of the continuum radiation transfer to high-speed re-entry vehicles or in simulation devices. It is of scientific interest because it is also sufficiently nonhydrogen like to allow some insight into those theories which aim at predicting the continuum for nonhydrogen systems. While no attempts were made to compare our data with all the theories which presently exist, a comparison has been made with those[4,5] which are currently in popular acceptance and use.

## EXPERIMENTAL APPARATUS AND TECHNIQUES

The details of the plasma generator and power supply have been discussed at length in previous work.[1,6,7] Only a brief description of its essential aspects will be presented here. The nitrogen plasma was generated by a mechanically constricted dc arc generator of the Gerdien type. Two different observing techniques were used; side on or perpendicular to the arc column, and end on along its axis.

For wavelengths greater than 2500 Å the arc was viewed side on and the data was gathered as a function of temperature by making use of the radial temperature variation of the arc column. The nitrogen test gas was confined to the central arc sections while the electrodes were blanketed in argon. Care was taken not to allow any of the argon to diffuse into the test region where spectroscopic measurements were made. These side-on intensities were converted to radial intensities by means of a numerical solution to the Abel integral as proposed by Barr.[8] For these measure-

ments an image of the arc or standard source was focused onto the slits of the spectrometer with front surface mirrors. Two instruments were used for making spectroscopic measurements for $\lambda > 2500$ Å; a Jarrell-Ash 0.5-m grating instrument with a dispersion of 16 Å/mm which was used for scans of the spectrum $\lambda > 2500$ Å and for the bulk of our temperature and continuum radiation measurements, and a Perkin-Elmer double-pass monochromator used for the infrared radiation detection.

Intensity measurements for $\lambda > 2500$ Å have been based on a tungsten-ribbon filament lamp calibrated by the National Bureau of Standards. For the data at 3.7 $\mu$ however, for which no calibration of the lamp was available, a silicon carbide "globar" was used as the standard radiation source.[9] For the near ultraviolet, 2500 Å, and blue part of the spectrum an EMI 6255B photomultiplier detector was used and for the red wavelengths a cooled RCA 7102 detector.

For wavelengths shorter than 2500 Å the arc was viewed end on and the temperature was varied by adjusting the power input to the arc.[10] In these measurements the plasma was essentially an argon arc to which a controlled percentage of nitrogen was added at the center of the column making sure that none of the nitrogen escaped to the electrode regions. The quantity of test gas added was limited to an amount that did not significantly change the temperature distribution established by the noble gas and such that the nitrogen gas was optically thin. In this manner it was possible to observe the nitrogen emission spectrum from an isothermal plasma to a wavelength of approximately 900 Å before strong absorption due to the argon ground state set in.

For this wavelength region a $\frac{1}{2}$-m Seya-Namioka spectrometer was connected to the end of the generator through a set of pin-hole apertures that limited the field of view to the axis of the discharge, and the radiation from the arc axis or standard source was viewed directly by the spectrometer. These baffles also serve as part of a differential pumping system that permitted the arc to run at atmospheric pressure while the spectrometer operated at $5\times10^{-6}$ mm Hg. A second spectrometer of a $\frac{1}{2}$-m Ebert design was positioned also end on to make temperature and concentration measurements from lines in the visible part of the spectral region. For these measurements light from the pin-hole apertures was directed into the second spectrometer by means of a diagonal mirror inserted in the optical path behind the apertures thus permitting both spectrometers to view the same element of plasma.

The detector used with the Seya was either a windowless photomultiplier or an EMI 6255B coated with sodium salicylate. The calibration of the detecting system for absolute intensity measurements was made using atomic nitrogen and hydrogen lines which were made to radiate like black bodies by increasing the test-gas concentration until the lines became optically thick. Intensity calibrations for the wavelengths at which the continuum was measured were taken from an interpolation of these line data.

In making intensity measurements careful attention was given to eliminate scattered light and the interference from second-order contributions, by the use of interference and Corning glass color filters. For example, for the 2500 Å data an interference-reflection filter with a bandpass of approximately 200 Å was used to prevent interference from scattered light, which would be particularly harmful at this wavelength because of the low-standard lamp signals. For $\lambda < 2500$ Å the amount of scattered light in the system was determined at the wavelengths where strong absorption from the two resonance argon lines 1066 Å and 1048 Å appeared. Estimates for the scattered light using this absorption region showed that its contribution was less than 5%. In all cases, measurements of the continuum radiation were taken in regions of the spectrum which exhibited a minimum contribution from line radiation.

For the vacuum ultraviolet the absorption coefficients of nitrogen in some cases were large enough to permit direct absorption measurements. These data were gathered by running two end-on arcs in tandem using one of them as a source. The calculation of the absorption coefficient was made from the following relationship:

$$(I_s - I_1)/I_2 = \exp(-\alpha L), \tag{1}$$

where $L$ is the path length through arc 1, $I_s$ is the sum of intensity from both arcs, $I_1$ is the intensity of the first arc, $I_2$ is the intensity of the second arc, and $\alpha$ is the absorption coefficient.

## TEMPERATURE AND NUMBER DENSITY MEASUREMENTS

The temperature of the nitrogen arc for $\lambda > 2500$ Å was determined from the continuum radiation at 4955 Å. The temperature dependence of the continuum at this wavelength was calibrated against the temperature variation of the absolute intensity of the 4935 N I line. This calibration procedure is discussed in detail in a previous paper,[1] as are all the corrections applied to the measured absolute line intensity.

The transition probability, $A$, selected for this multiplet was $2.34\times10^{6}$ sec$^{-1}$ as recommended in the National Bureau of Standards (NBS) tables.[11] We had previously[1] used a value of $1.93\times10^{6}$ sec$^{-1}$ which was calculated from the Bates and Damgaard[12] tables. We found on close inspection of

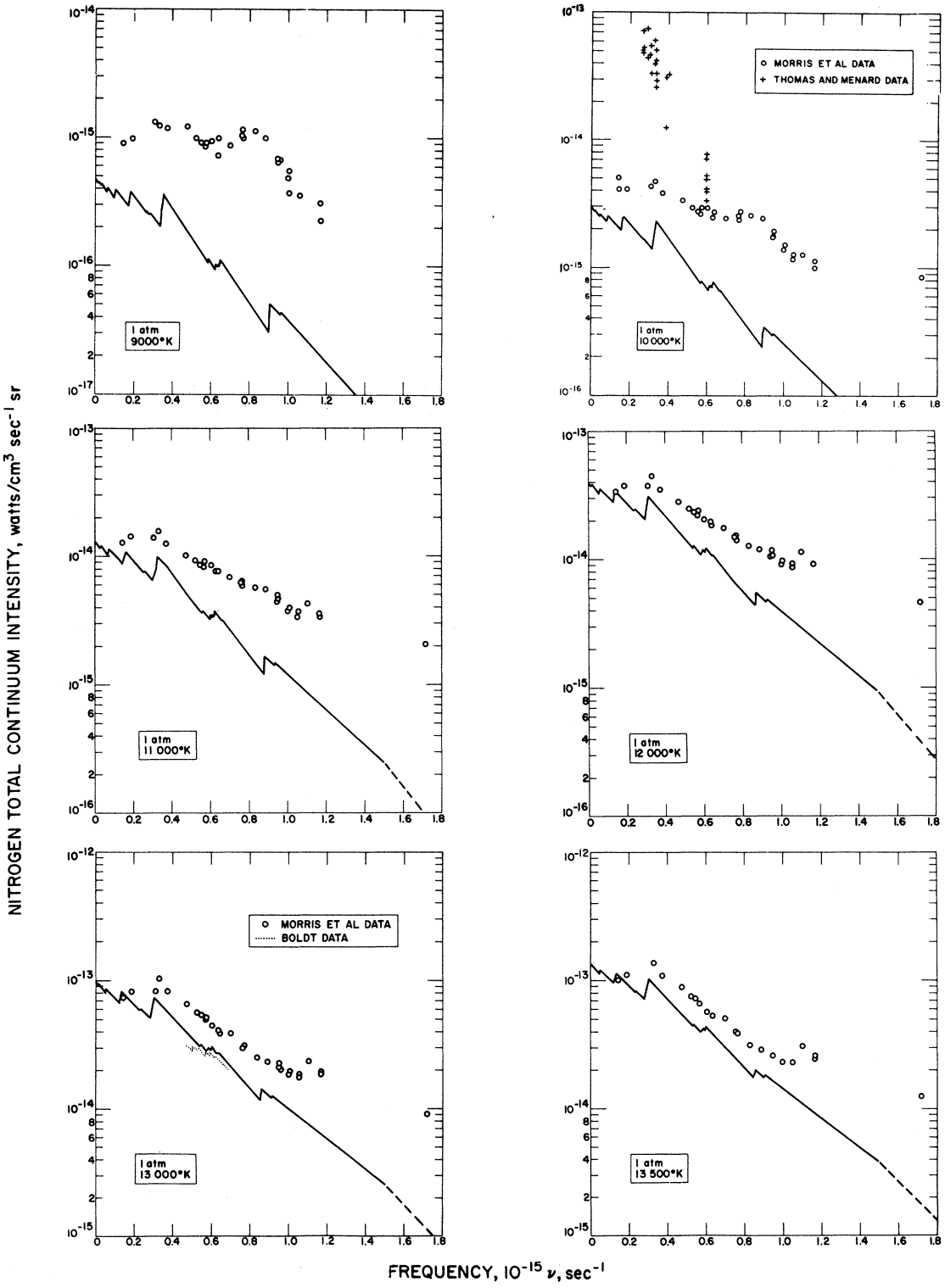


FIG. 1. Spectral distribution of the nitrogen experimental total continuum intensity at atmospheric pressure. Comparison is made to the experimental data of Thomas and Menard at 10 000° K and Boldt at 13 000° K. The solid line is the contribution of positive-ion radiation ($I_{fb+ff^+}$) calculated with recombination cross sections found from Burgess and Seaton's quantum-defect method and from the free-free Gaunt factors of Karzas and Latter.

these calculations that 4935 N I belonged to that class of lines covered in the tables that gave $A$ values quite sensitive to small errors in the upper and lower energy values used for the calculations. New experimental measurements at higher temperatures than had previously been obtained showed that the measured maximum intensity of 4935 N I exceeds the theoretically calculated values using an $A$ value of $1.93\times10^{6}$ sec$^{-1}$. This clearly indicated that this value was too small. Of the experimental values available to us, the one suggested in the NBS tables appeared to be most reliable. Temperatures were also measured using the 5045 N II line. These results were found to be in good agreement with the 4935 N I measurements. The $A$ value of the ionic line was calculated from the Bates and Damgaard tables. It did not suffer from the same difficulties as 4935 N I and in fact, could be determined with a precision of better than a few percent.

Temperatures of the end-on argon-nitrogen arc used for the vacuum uv work were found from two argon lines and their adjacent continua: 4300 A I and 4806 A II, and the continuum at 4315 and 4820 Å, respectively. The half-widths selected were those of Popenoe[13] who made the experimental calibration using $H_\beta$ as the electron number density indicator. The transition probabilities used for these lines were $3.6\times10^{5}$ sec$^{-1}$ for the atomic line and $1.1\times10^{8}$ for the ionic line. These values represent a choice which gives the most consistent agreement to data for intensity and electron number density measurements made by four laboratories, ours, Shumaker's,[13] Richter's,[14] and Olsen's.[15] These data covered pressures ranging from 0.5 to 5.0 atm and used both side-on and end-on techniques for arcs of different sizes and power inputs.

It should be stated here that in all our calculations for nitrogen and argon, the composition and partition-function tables of Drellishak[16] were used. For the vacuum ultraviolet studies on argon plasmas and the corresponding nitrogen mixture we used our own density calculations. The latter did not employ a lowering of the ionization energy.

The number of test-gas atoms per unit volume on the axis of the arc used in the vacuum ultraviolet studies was measured for nitrogen from the absolute intensity of the 4914 N I and 7424 N I lines. The relationship connecting this intensity measurement with the number of atoms is

$$N^0 = I4\pi\lambda U^0[\exp(E_i/KT)]/hcgA\,, \qquad (2)$$

where $N^0$ is the atom number density, $\lambda$ is the wavelength of the spectral line, $U^0$ is the atom partition function, $E_i$ is the upper-level energy value, $K$ is the Boltzman constant, $T$ is the temperature, $h$ is Plank's constant, $c$ is the velocity of light, $g$ is the statistical weight of the upper level, and $A$ is the transition probability.

An uncertainty in temperature of ±250°K results in an error of ±7% in the nitrogen-atom concentration. Adding to this a ±15% error in the intensity measurement and uncertainty in the transition probability gives a total error of about ±22%. Measurements of the nitrogen concentration using the above technique gave values which agreed within experimental error with the original ratio of the nitrogen-argon mixture added to the arc.

## CONTINUUM MEASUREMENTS

Nitrogen continuum radiation measurements were taken at 1- and 2-atm pressure for a wavelength range extending from 900 Å in the vacuum ultraviolet to 37 000 Å in the infrared. These data are divided up into two wavelength intervals for presentation. The wavelengths from 2500 to 37 000 Å are presented in Figs. 1 and 2 for 1- and 2-atm pressure, respectively. A comparison of the two sets of data showed no anomalous pressure dependence. The continuum measurements shown for $\lambda > 2500$ were made using the "side-on" method for currents of 30, 40, and 50 A. These data were taken using a spectrometer bandpass ranging from 4 to 10 Å for $\lambda < 12\,000$ Å and 100 to 400 Å for $\lambda > 12\,000$ Å. Figures 3 through 7 give spectral scans showing the wavelengths selected for measurement (indicated by arrows). These figures show the spectral structure in the neighboring wavelength regions. Figures 8 and 9 give the continuum data for the vacuum uv in terms of absorption coefficients. Included in these figures are the data from both the emission and direct absorption measurements. Figure 10 gives the temperature dependence for two wavelengths 975 and 1112 Å in the vacuum ultraviolet. Also included in Figs. 1, 2, 8, 9, and 10, are theoretical predictions for the nitrogen positive-ion radiation. The analytical calculations are presented in detail in the Appendix, and the comparison of our data to these theoretical estimates are discussed later in the paper.

## ACCURACY AND COMPARISON OF EXPERIMENTAL DATA

The accuracy of the measured continuum data varies with frequency and temperature. For $\lambda > 2500$ Å at the higher temperatures and in the middle of the frequency range covered where the standard lamp and arc signals are highest and the phototubes have maximum sensitivity, the values should be good to ±10%. Under the worst conditions for the photocell measurements, say 9000°K and at the ends of the frequency range, for the side-on data the measurements are

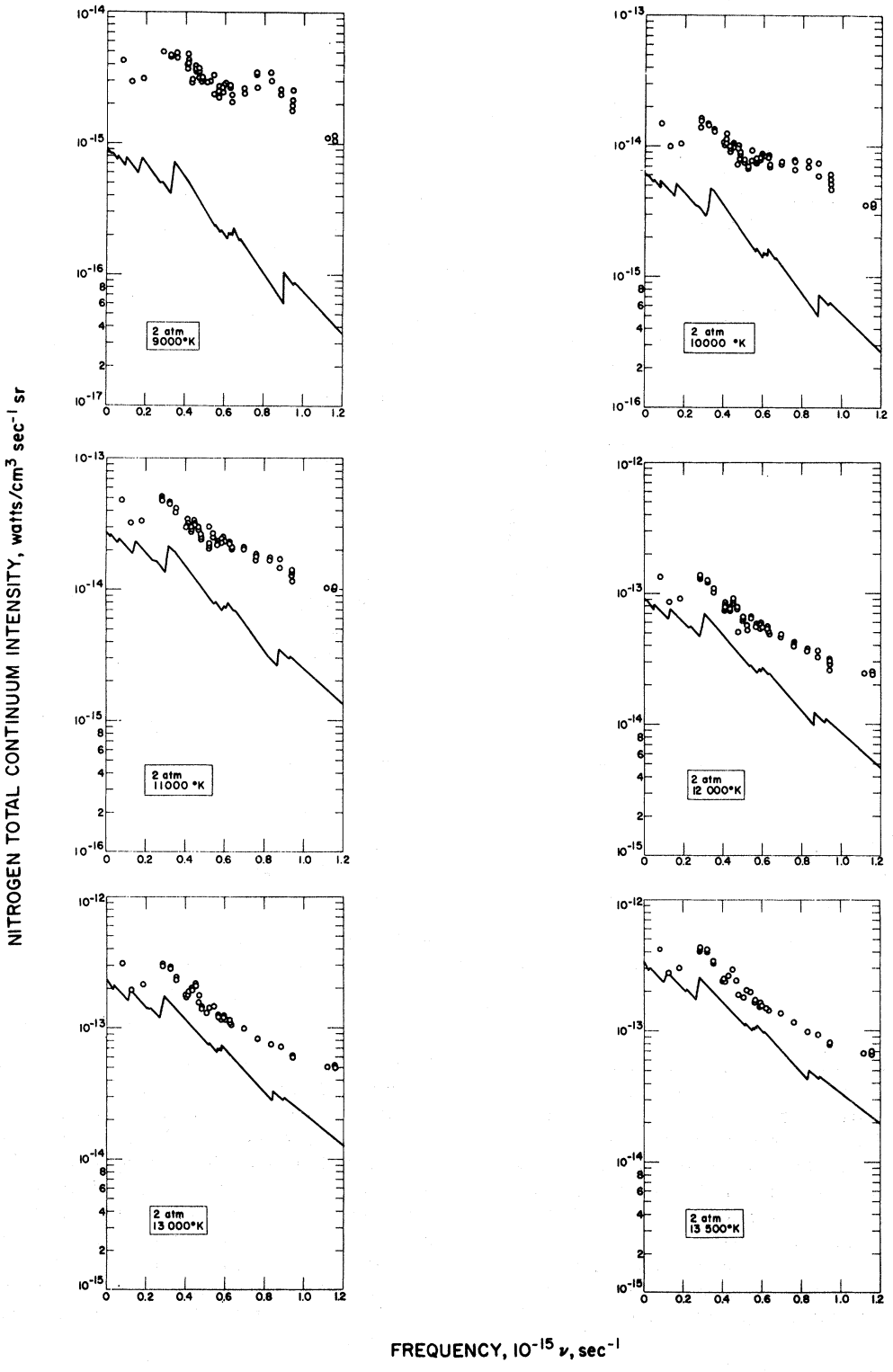


FIG. 2. Spectral distribution of the nitrogen experimental total continuum intensity at 2-atm pressure. The solid line is the contribution of the positive ion radiation ($I_{fb+ff^+}$) calculated from recombination cross sections found from Burgess and Seaton's quantum-defect method and from the free-free Gaunt factors of Karzas and Latter.

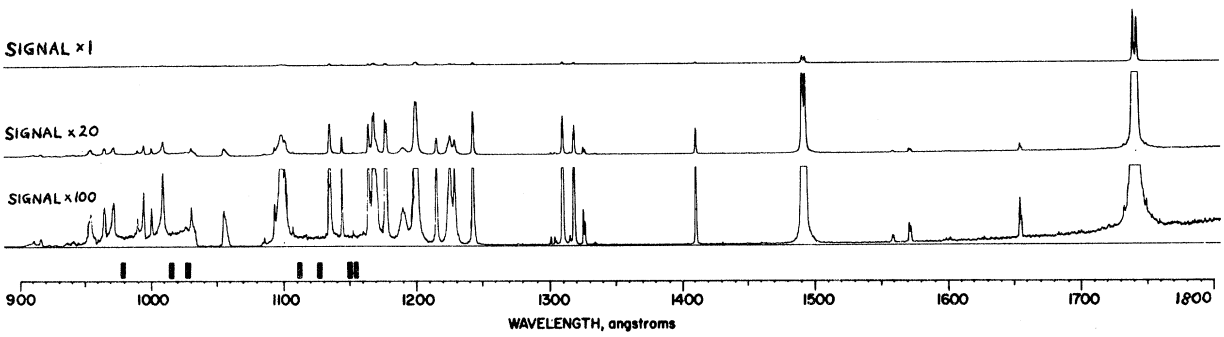


FIG. 3. Vacuum ultraviolet spectral scan of a nitrogen-argon plasma taken end-on at atmospheric pressure and at about 13 600°K. The solid bars show the wavelengths at which continuum radiation measurements were made.

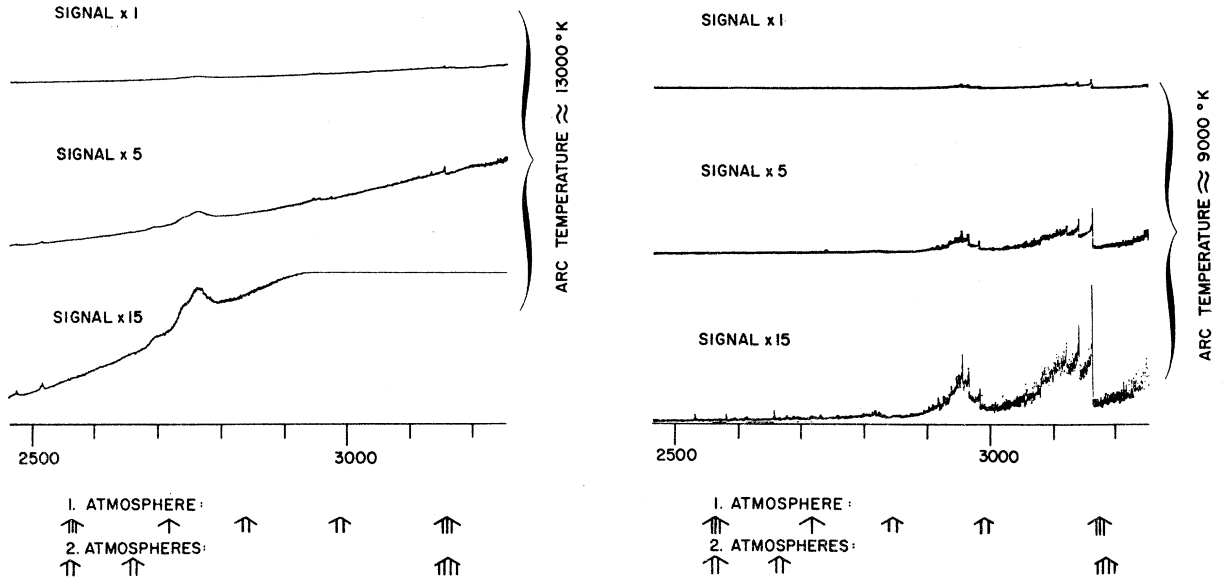


FIG. 4. Side-on spectral scan of a 1-atm nitrogen arc taken at the center and at the outside edge for a wavelength interval from 2500 to 3250 Å. The arrows indicate the wavelengths at which 1- and 2-atm data were obtained.

probably good to ±30%. These estimates do not include effects arising from inaccuracies in transition probabilities of the line used for calibrating the 4955 Å continuum versus temperature. Neither do they include errors in composition calculations such as the lowering of the ionization energy or the partition-function cutoff. Errors from these parameters are difficult to assess and at best an educated guess might put an additional 15% deviation on the intensity measurements. The spectral intensity for the 1743 Å (or $1.72\times10^{15}$ sec$^{-1}$) 1-atm data is seen to be about a factor of 10 greater than theory at 13 500°K. We are less confident in these radiation measurements and their temperature dependence since it was not possible to obtain an accurate estimate for scattered light.

The emission data for $\lambda < 1500$ Å we believe to have an absolute accuracy of ±40%. This has been estimated from the combined effects of scatter in the data, errors in temperature and concentration measurements, and the quality of the blackbody line intensities used as the radiation standard. The accuracy of the direct absorption measurements in the vacuum ultraviolet data is quite low for the wavelengths of lowest absorption because the differences $I_s - I_1$ in Eq. (1) were small. Within the accuracy of the measurements however, the data confirm the emission measurements.

All of the tests for local thermodynamic equilibrium suggested by Griem[17] were applied to the conditions reached in our arc and were found to be fulfilled. Of the criteria that Griem lists, one of the most important in the analysis of our data is that there be an equilibrium population of the

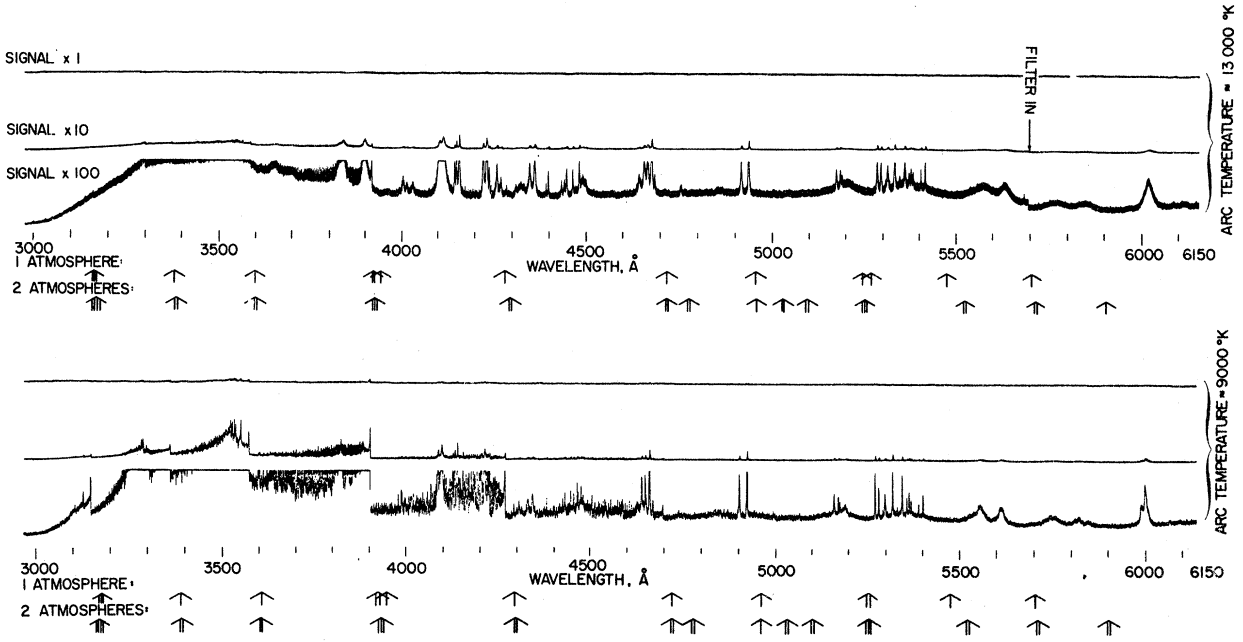


FIG. 5. Side-on spectral scan of a 1-atmosphere nitrogen arc taken at the center and at the outside edge for a wavelength interval from 3000 to 6150 Å. The arrows indicate the wavelength at which 1- and 2-atm data were taken.

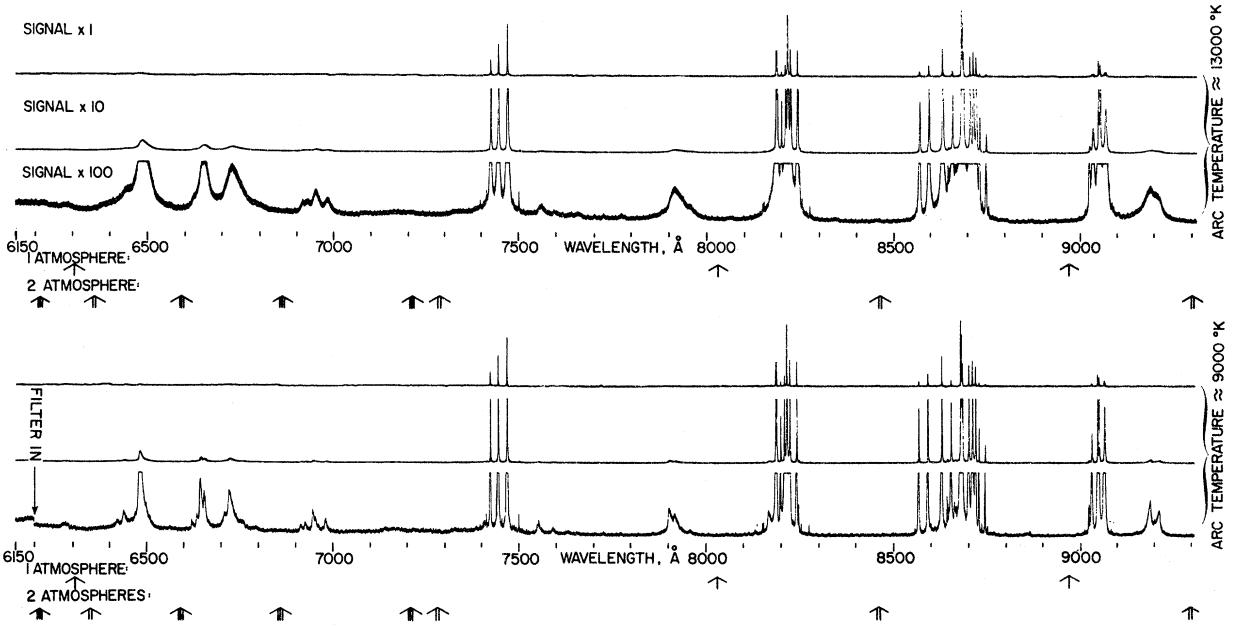


FIG. 6. Side-on spectral scan of a 1-atm nitrogen arc taken at the center and at the outside edge for a wavelength interval from 6150 to 9300 Å. The arrows indicate the wavelength at which 1- and 2-atm data were taken.

ground and first-two excited states of the atom since these levels form the parent terms of the nitrogen negative ions. It was possible to experimentally check the population of these levels with the absorption measurements discussed above. From these measurements we found that within a factor of 2 the population of these levels indeed follows a Boltzman distribution. More details concerning equilibrium are further discussed under the neutral-atom radiation paragraphs.

In comparing our data for $\lambda > 2500$ Å with other experimental results, we find at 13 000°K an intensity higher than Boldt's[18] by a factor of 2. We

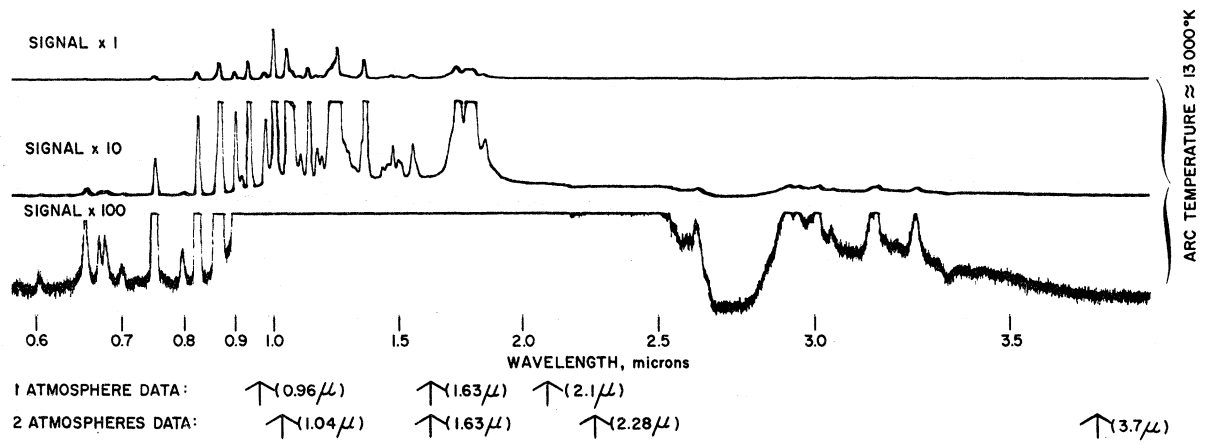


FIG. 7. Side-on spectral scan of a 1-atm nitrogen arc taken at the center for a wavelength interval from 0.6 to 3.7 $\mu$. The arrows indicate the wavelengths at which 1- and 2-atm data were obtained.

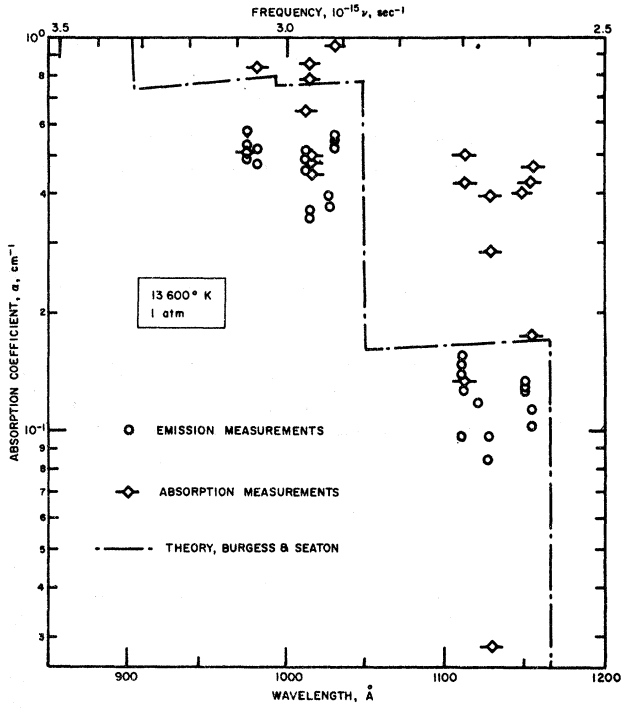


FIG. 8. The absorption coefficient of the nitrogen vacuum uv continuum at atmospheric pressure determined from both emission and absorption measurements. Comparison is made to the theory (dot dashed line) using Burgess and Seaton's quantum-defect method for calculating recombination cross sections.

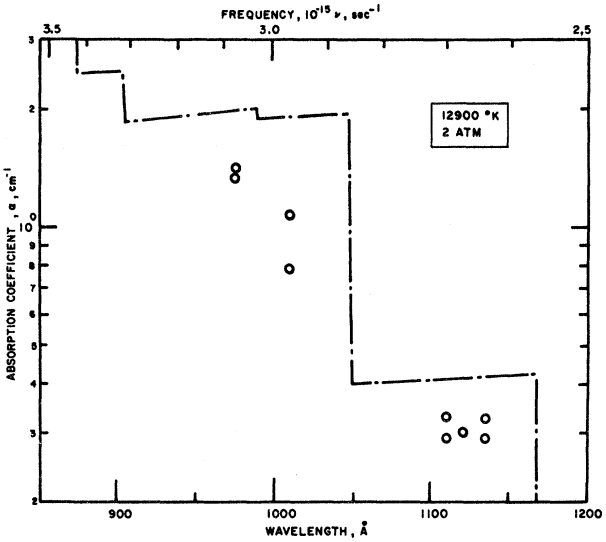


FIG. 9. The absorption coefficient of the nitrogen vacuum uv continuum at 2-atm pressure as found by emission measurements. Comparison is made to the theory (dot dashed line) using Burgess and Seaton's quantum-defect method for calculating recombination cross sections.

believe that part of this factor may be due to differences in the transition probabilities chosen for the spectral lines used for temperature measurements as well as differences in the calculations for the plasma composition.

A comparison of our results with that of Thomas[19] for 10 000°K shows his data to be higher than ours by a factor of 2 at 5000 Å and by as much as a factor of 20 at 11 000 Å. We do not know why this difference exists. The significance of this difference however is discussed in the neutral-atom radiation section.

## SEPARATION OF THE CONTINUUM INTO $N^+$ AND $N^0$ CONTRIBUTIONS

For our experimental conditions of temperature and pressures we have considered that the continuum radiation of nitrogen results from two species interacting with electrons; positive ions

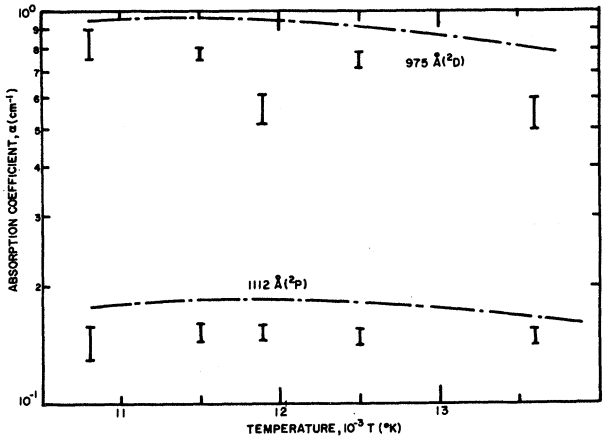


FIG. 10. The vacuum uv continuum absorption coefficient at two wavelengths of nitrogen versus temperature for a 1-atm plasma pressure. The dash dot curve is theory using Burgess and Seaton's quantum-defect method for calculating recombination cross sections.

and neutral atoms. Each of these species interacts with electrons by means of two mechanisms: the free-free or Bremsstrahlung radiation process and the free-bound or recombination radiation process. The total continuum radiation of nitrogen at a wavelength, $\lambda$, can be expressed as the sum of these continua:

$$I_\lambda(\text{total}) = I_{\text{fb}}{}^{+} + I_{\text{ff}}{}^{+} + I_{\text{fb}}{}^{0} + I_{\text{ff}}{}^{0}. \tag{3}$$

To study the radiation from $N^+$ and $N^0$ we have provided a separation of these continua. To do this we used the temperature dependence of the respective processes to obtain the $N^+$ radiation and a subtraction technique to obtain the $N^0$ radiation. The "temperature-dependence" method was successfully applied in analyzing our oxygen continuum measurements[6] and the resulting negative-ion cross sections and estimates for the positive-ion radiation gave good agreement with other experimental results and also with theory. It was felt therefore that this analysis technique could be applied to nitrogen with confidence. The method is briefly reviewed here along with the revisions made to obtain more precise values for the neutral-atom radiation. It should be noted here that this scheme is only applied to the data for $\lambda > 2500$ Å since in the vacuum uv all the radiation is due to $N^+$ free-bound radiation.

The equation relating the contribution of the continuum from both the free-free and free-bound collision of electrons with a given species $i$ is

$$I_{\text{ff+fb}}{}^{i} = 5.443\times10^{-46} Z^2 g N^i N_e T^{-\frac{1}{2}} e^{-C_2/\lambda T} + 40.03\times10^{-24} (e^{-C_2/\lambda T}/\lambda^3) \sum \sigma_{nlj} N_{nlj}{}^{i-1} \quad (\text{W/cm}^3\,\text{sec}^{-1}\,\text{sr}), \tag{4}$$

where the first term represents the simple Kramers[20] expression for bremsstrahlung or free-free radiation and the second gives the recombination radiation process. In this case $i$ designates either the nitrogen ions or atoms reacting with electrons, $N^i$ is the species number density, $N_e$ is the electron number density, $Z$ is effective nuclear charge, $g$ is the gaunt factor, $C_2$ is the second-radiation constant, $N_{nlj}{}^{i-1}$ is the number density for the level $nlj$ of the species corresponding to $i-1$, and $\sigma_{nlj}$ is the photoabsorption cross section corresponding to the $nlj$ level of the $i-1$ species.

For the positive ion-electron radiating process we chose to use theoretically calculated cross sections in Eq. (4) and fit the resulting estimate for $I_{\text{ff+fb}}{}^{+}$ to our experimental data. These calculations are described in detail in the Appendix. Briefly, however, the calculations were made with the following input: For the recombination radiation for $\lambda > 2500$ Å we used the cross sections calculated by Griem[17] who made a modification to the quantum-defect work of Burgess and Seaton.[4] For terms of principal quantum numbers 4 and higher the hydrogen cross sections were employed. For the free-free radiation mechanisms the Gaunt factors of Karzas and Latter[5] were used.

For the neutral atom-electron interaction there are no theoretical values for $\sigma_{N^-}$ available, therefore we let this term be the unknown in Eq. (4) and simplified the free-bound expression by solving for the cross section of the negative-ion state that is the predominant radiation contributor in the spectral region where our measurements lie, namely that corresponding to the $^1D$ negative ion. Reasons for this choice are discussed in a following section. Under this condition the free-bound term for the neutrals in Eq. (4) reduces to

$$I_{\text{fb}}(N^0) = 40.03\times10^{-24} \times (e^{-C_2/\lambda T})\sigma_{^1D} N_{^1D}{}^{-}/\lambda^3 \tag{5}$$

and the two unknowns to be determined for this radiation mechanism are therefore, the $\sigma_{^1D}$ for the free-bound radiation, and the $Z^2 g$ for the free-free process.

The total radiation for both the positive ion and neutral atom at wavelength $\lambda$ can thus be expressed as:

$$I_\lambda(\text{total}) = R I_{\text{theory}}{}^{+}$$

$$+\sigma_{^1D} I_{fb}{}^0/\sigma_{^1D} + Z^2 g I_{ff}{}^0/Z^2 g\,, \qquad (6)$$

where $I_{\text{theory}}{}^+$ is the theoretical prediction for the ff and fb radiation of positive ions reacting with electrons, (see Appendix), $R$ is the factor by which our experimental data must be multiplied to fit the theoretical estimates for the $I_{\text{theory}}{}^+$ radiation, $I_{fb}{}^0$ is the free-bound radiation of neutrals reacting with electrons [Eq. (5)], $Z^2 g$ is an unknown for the neutral-atom free-free process, $\sigma_{^1D}$ is the photo-ionization cross-section of the neutral nitrogen atom, and $I_{ff}{}^0$ is the free-free radiation of neutrals reacting with electrons. In principal for each wavelength $\lambda$, Eq. (6) could be solved simultaneously for $R$, $\sigma_{^1D}$, and $Z^2 g$ using experimental data at three temperatures. However, the free-free and free-bound terms for the neutral-atom radiation have practically the same temperature dependence, making it impractical to simultaneously extract $\sigma$ and $Z^2 g$ by this method. It was therefore decided to treat the neutral atom radiation as either all free free or all free bound and make only a two-term fit to the data of the following types:

$$I(\lambda) = R I_{\text{theory}}{}^+ + \sigma_{^1D} I_{fb}{}^0/\sigma_{^1D}\,, \qquad (7)$$

and

$$I(\lambda) = R I_{\text{theory}}{}^+ + Z^2 g I_{ff}{}^0/Z^2 g\,. \qquad (8)$$

The latter curve fit, Eq. (8), yields values of $Z^2 g$ which have a frequency dependence such that when extrapolated to the infrared yields the $Z^2 g$ value for the pure free-free radiation.

## COMPARISON AND CONCLUSION FOR THE $N^+$ CONTINUUM RADIATION

The comparison of the $N^+$ ff and fb continuum radiation with theory is shown in Fig. 11 where the ratio $R$ of experiment to theory is given versus $\lambda$ and $\nu$. This comparison is made for both 1 and 2 atm. No significant pressure dependence is observed. Figure 12 shows a typical curve fit at 4955 Å using the temperature-dependence separation technique. These data show that the fit adequately accounts for all the radiation and that the $R$ values are not sensitive to the temperature selected for the fit. The $R$ values therefore have about the same accuracy as the high-temperature continuum measurements and thus provide good estimates of a correction factor to make the theoretical estimates for the positive-ion radiation agree with experiment.

An examination of the $R$ values versus wavelength gives some information as to the agreement of theory and experiment for the cross sections of the various energy levels of nitrogen (see Appendix). For example in the vacuum ultraviolet the two levels that are the dominant contributors to our measured radiation are the $2p^3\,{}^2P$ and $2p^3\,{}^2D$, with the free-bound process being the predominant mechanism and little radiation coming from the ff processes. Since we believe the accuracy of our data in these regions to be $\pm 40\%$ we can say that there is essentially agreement between theory and experiment. This of course supports Hahne's[21] calculation of the cross section in the vacuum uv using the quantum-defect method of Burgess and Seaton (see Appendix).

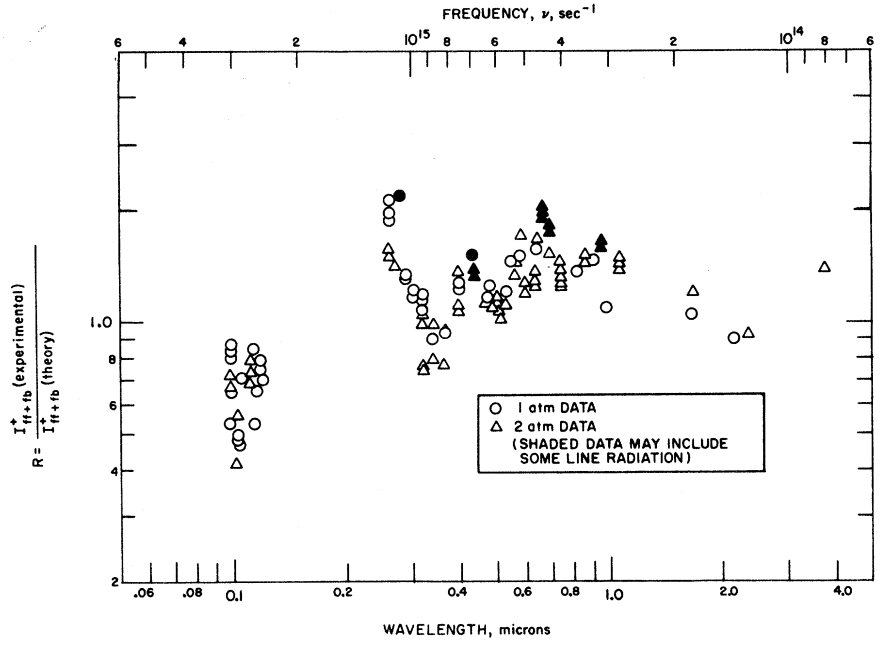


FIG. 11. The ratio $R$ of our experimental values of the free-free and free-bound ($I_{ff+fb}{}^+$) radiation for the nitrogen positive ion to the theoretical values predicted using Burgess and Seaton's quantum-defect method for calculating recombination cross sections and Karzas and Latter's free-free Gaunt factors.

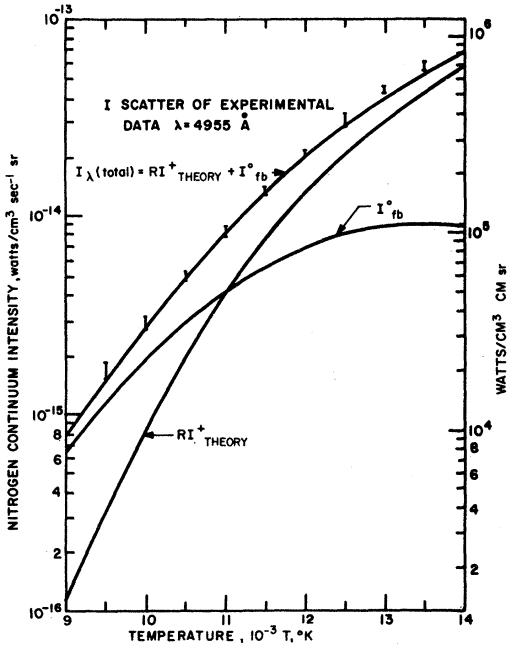


FIG. 12. Estimates of the positive-ion ($RI_{\text{theory}}^{+}$) and negative-ion ($I_{\text{fb}}^{0}$) contributions to the total measured nitrogen 1-atm 4955 Å continuum radiation as found from the temperature-dependence curve fit.

For wavelengths greater than 2500 Å we have used the cross sections suggested by Griem,[17] calculated using the quantum-defect method, for levels falling between 2000 and 6000 Å and hydrogen cross section for levels lying at greater wavelengths. We find in the 2500 to 3000 Å region, where the $3s^2P$ and $3s^4P$ levels are prominent, that the measured values are much higher than theory with the difference being frequency dependent. Since this difference is greater than the experimental error believed to be associated with these data it suggests that the cross sections for these levels are too low, in the worst case perhaps by a factor of almost two, or that there may be levels missing in the calculation. In the 4000 to 10 000 Å region the data tend to go higher than theory with increasing wavelength. This has suggested to us that the starting point for using hydrogen cross sections with levels of principal quantum number of four may be premature. Beyond 10 000 Å the data supports within the limits of error the use of hydrogen cross sections, the inclusion of prime terms, as well as the ff gaunt factors of Karzas and Latter.[5]

In conclusion then for the $N^+$ radiation it is fair to say that over a large portion of the wavelength region studied our data supports the use of the quantum-defect method of Burgess and Seaton for calculating the energy transferred by continuum radiation in a plasma. However, it is obvious that if the continuum is to be used as a diagnostic tool such as electron concentration or temperature measurements some care should be used in selecting the wavelength to be used.

## NEUTRAL-ATOM CONTINUUM RADIATION

Our data and that of other investigators, Boldt[18] and Thomas[19] show that there is considerable radiation from nitrogen which cannot be accounted for by the $N^+$ processes and which exhibits the temperature dependence of the free-free and free-bound radiation of the neutral nitrogen atom. There is some controversy over the origin of this radiation. This controversy[18,19,22,23] arises principally because there are no suitable wave functions and ionization energies to obtain reliable theoretical predictions necessary to support or refute the existence of the nitrogen negative ion and the magnitude of its cross section. Below we present arguments, based on the character of our experimental data, to support the existence of this ion. We also present an analysis of the experimental data to obtain the principal states of $N^-$ responsible for the bulk of the radiation. It suggests upper and lower limits for the ionization energies of these states and also tests the validity of the observed magnitude of the experimental cross section by an application of the sum rule. Finally, we list supporting arguments which through analogy to similar data of oxygen and argon give some confidence to the conclusions reached.

From an evaluation of the $\sigma$ values found from the temperature-dependence separation technique we found that unlike the $R$ values, the corresponding cross sections were very sensitive to small changes in the lower temperature chosen for the curve fit, and that not all the measured radiation would always be accounted for at the lower temperatures. Therefore for the analysis of the neutral-atom species we subtracted from the total measured continuum at 9000°K the contribution from the positive ions. The latter contribution was determined from the theoretical continuum for $I_{\text{ff}+\text{fb}}^{+}$ times the experimental correction factor, $R$, obtained from the curve-fit method. The resulting radiation is shown in Fig. 13. No attempt was made to extrapolate the 1743 Å continuum data to 9000°K since its precision did not warrant it. In order to give us the maximum use of all the data, the 1- and 2-atm values were normalized at 4955 Å. Both sets of data are plotted in the figure. These data were reduced to a smooth curve by taking the average value of two envelopes, drawn through the maximum and the minimum points.

For the free-free neutral-atom radiation the $Z^2g$ was derived from the curve fit using Eq. (8). It is noted that in solving for this value of $Z^2g$, we assumed the measured $Z^2g$ would have a fre-

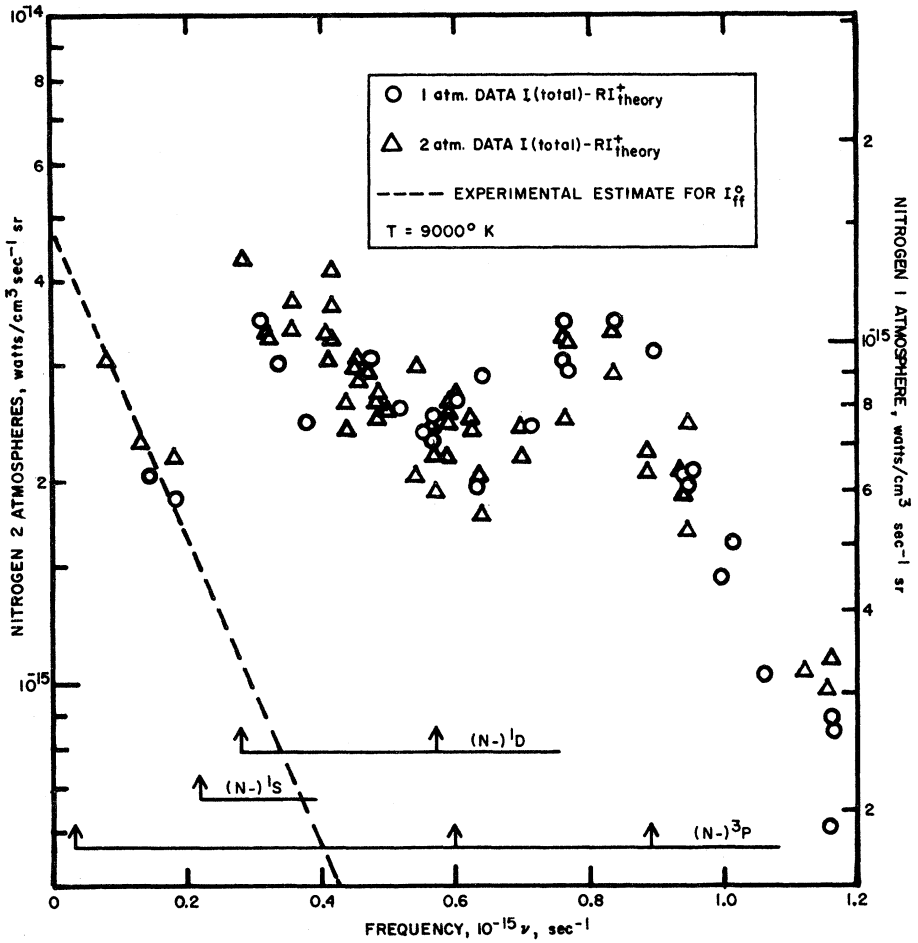


FIG. 13. Nitrogen 1- and 2-atm neutral-atom radiation at 9000°K as found by subtracting the positive-ion contribution ($RI_{\text{theory}}^{+}$) from the total measured continuum data. The arrows indicate the position of the negative-ion absorption edges using the ionization energies shown in Fig. 15.

quency dependence such that when extrapolated to the infrared frequencies would yield the $Z^2g$ value for the pure free-free radiation. Figure 14 plots the results of the $Z^2g$ values found by this fit for both 1- and 2-atm nitrogen data and also shows the values obtained by Taylor[24] in the infrared. His values are seen to be lower than ours by about a factor of 2, but are believed to agree within the experimental error of both data. We chose to use our average experimental $Z^2g$ of 0.052 to subtract the neutral free-free radiation from the data in Fig. 13.

The remaining radiation for $\nu > 0.20\times10^{15}$ which is presumably due to neutral atom-electron recombinations shows two absorption edges, one between 0.2 and $0.3\times10^{15}$ and the other around $0.6\times10^{15}$ sec$^{-1}$. Assuming that the largest contributor to the absorption for these conditions is the negative ion of nitrogen, we can make use of a combination of the term diagram, Fig. 15, and the composition calculations, Fig. 16, to find a model that suitably explains the absorption edges. The energy levels and the respective $\Delta E$'s of the negative ions shown in Fig. 15 were constructed from theoretical values for the ionization energies and from the absorption-edge structure in our data. Using the ionization energies shown in the figure, the approximate frequency of the edges corresponding to the $^1S$, $^1D$, and $^3P$ levels are indicated in Fig. 13.

In trying to assign the neutral-atom radiation to the proper negative ion, one might attempt to first fit the $^3P$ ground state to the data. Theoretical values[25–31] for the possible ionization energies of this negative-ion range from − 0.15 to + 0.54 eV. If one uses an ionization energy of 0.1 eV[25] as shown in Fig. 15 then clearly the absorption edge that should fall around $0.89\times10^{+15}$ sec$^{-1}$ is not observed. By using a higher ionization energy, namely 0.54 eV[29] the $^3P$ edges fall at around $0.13\times10^{15}$, $0.71\times10^{15}$, and $1.00\times10^{15}$ sec$^{-1}$. If this is a respectable fit to the data, then a reasonable profile is obtained provided that (a) the radiation in the infrared ($\nu < 0.2\times10^{15}$ sec$^{-1}$) is not totally due to free-free neutral-atom radiation, and (b) that the high level of radiation at 1743 Å and 10 000°K, Fig. 1, is real and indicative of free-bound neutral-atom radia-

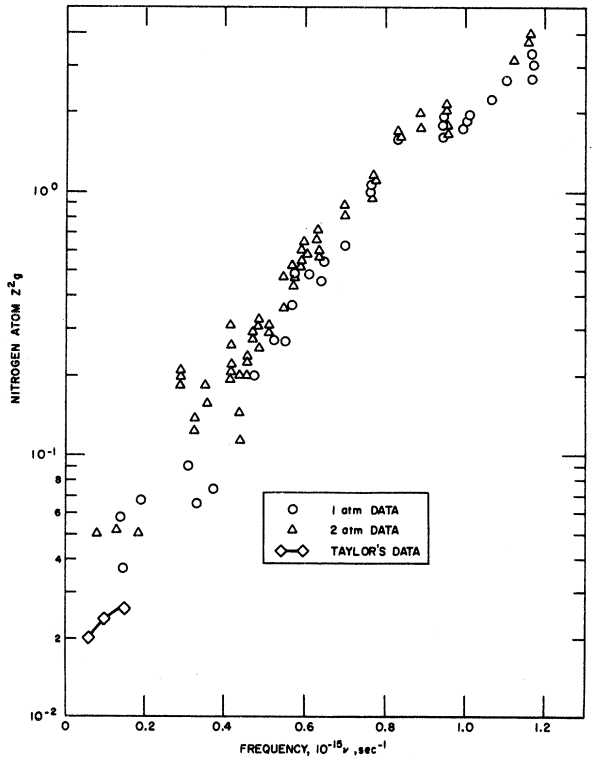


FIG. 14. Nitrogen $Z^2g$ values corresponding to the neutral-atom free-free process as obtained from the temperature dependence curve fit. Comparison is made to the experimental results of Taylor.

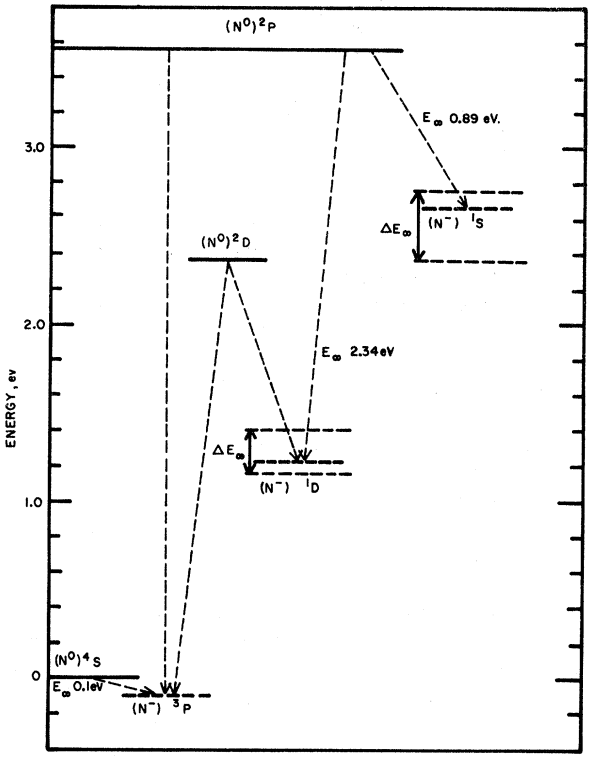


FIG. 15. Energy-level diagram for the nitrogen negative ions and their atomic parent terms. The $\Delta E_\infty$ ranges were found from our experimental data.

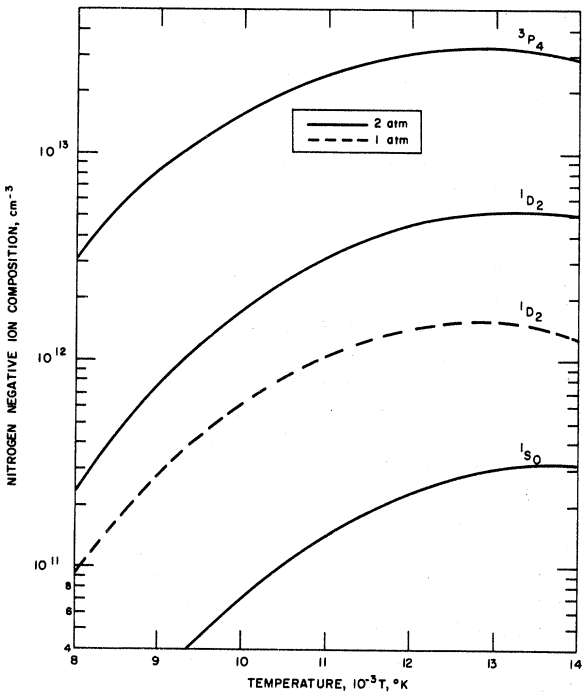


FIG. 16. Number density estimates for the three nitrogen negative ions calculated using the ionization energies shown in Fig. 15.

tion in the vacuum ultraviolet. As mentioned earlier, the reliability of the latter data does not warrant a positive assignment of another absorption edge between $1.2\times10^{15}$ and $1.72\times10^{15}$ $sec^{-1}$. More important however, is the fact that an ionization energy of 0.54 eV for the ground-state negative ion should indicate that the $^3P$ ion is stable and it would therefore seem that its existence would have been verified by now using the same techniques by which the oxygen negative ion has been measured. Little[32] or no such experimental evidence has been obtained thus far to substantiate its existence. From these arguments we assumed in this analysis that the $(N^-)$ $^3P$ ion is not a stable contributing source for the negative-ion radiation.

Using the same system of arguments as above leads us to believe that the $^1D$ nitrogen ion is a more reasonable explanation for the residual radiation. This level has a higher ionization energy and has therefore a more stable configuration. The ion is formed from two excited levels of $N^0$, the $^2P$ and $^2D$ states. Since it has two ionization limits it thus has two absorption edges. If the absorption edge due to a $^2P(N^0) \rightarrow {}^1D(N^-)$ transition falls around $0.6\times10^{15}$ $sec^{-1}$, then the second edge for the $^2D(N^0) \rightarrow {}^1D(N^-)$ transition must fall around $0.3\times10^{15}$ $sec^{-1}$. Inspection of

the data around these two frequencies shows that these edges can exist and furthermore the data allow us to give limits for the $^1D(N^-)$ energy level. These are shown in the term diagram, Fig. 15.

The ionization energy of 0.89 eV[23] for the $^1S$ term as shown in Fig. 15 would also give an edge near $0.3\times10^{15}$ sec$^{-1}$, a frequency that falls within the limits of the experimental edge. It does not appear however, that this term contributes significantly to the radiation since the concentration of the $^1S$ level is almost an order of magnitude lower than that of the $^1D$ which also has an edge in the same vicinity. We feel therefore that it is more reasonable to assume that this edge consists mainly of radiation to the $^1D$ state.

The cross sections which appear in Fig. 17 have therefore been calculated for the $^1D$ ion. Included in this figure are also the experimental estimates for the $^1D$ cross section as found by Boldt[18] also from arc measurements. We have not compared the cross section for the negative ion found by Thomas[19] since he reduced his data to a cross section for the ground state $(N^-)^3P$ using, incidentally, an incorrectly calculated partition function. However, if we take the liberty of converting his data to correspond to the $(N^-)^1D$ ion it would yield cross sections that are higher by an order of magnitude than ours at around 1.1 $\mu$. However, at 5000 Å he would have obtained a $^1D$ cross section which would agree with ours within the experimental accuracy of both sets of data.

*Note added in Proof*: Additional data for the cross sections of $N^-(^1D)$ have recently been published.[32a] They are found to be in good agreement with those reported in this paper. Reference (32a) states that we have not included all the $3p$ levels in our calculations for the nitrogen positive ion continuum. We refer them to the Appendix of this paper and to Figs. 1 and 2. We believe they will find that the levels have been treated correctly.

A test of the validity of the cross sections determined from our data for the $(N^-)^1D$ state can be made through an application of the sum rule.[33,34] This sum rule is given as

$$N=(mc/\pi e^2)\int_{\nu_0}^{\infty}\sigma(\nu)d\nu \ , \qquad (9)$$

where $\sigma(\nu)$ is the photo-ionization cross section of the state of interest as a function of frequency, $N$ is the number of electrons in the ion, which for $N^-$ is 8, and $\nu_0$ is the photo-ionization threshold. Integration of our experimental data gives about 10 electrons. Assuming a $1/\nu^3$ dependence for the cross section in the frequency range not included by the data, gives 2.5 additional electrons or a total of 12.5. This value is 50% higher than theory predicts for the $(N^-)^1D$ ion, however, we feel that it is within the combined errors of the data and the analysis.

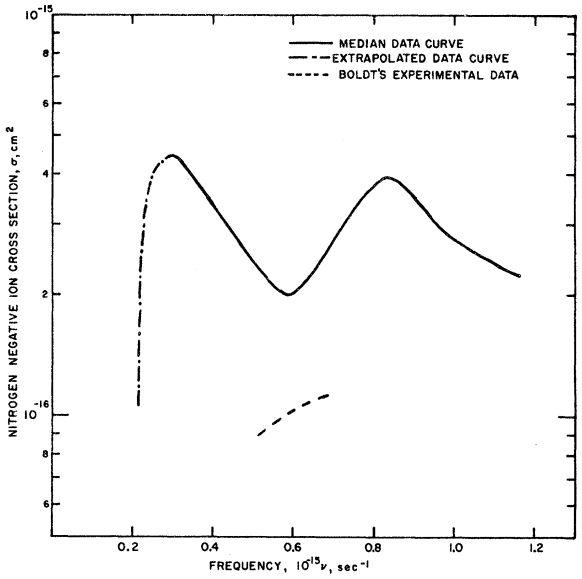


FIG. 17. Our experimental estimate for the nitrogen negative-ion cross section for the $^1D$ ion. Comparison is made to the experimental results of Boldt.

In looking for a possible explanation for some of the surplus electrons one could question whether there is an over population of the metastable $(N^0)^2P$ and $(N^0)^2D$ atomic nitrogen levels. This would give more $(N^-)^1D$ ions than predicted through the composition calculations and would result in our seeing too large a cross section. To determine if such an over population of the atomic $(N^0)^2P$ and $(N^0)^2D$ levels exists, we made absorption-coefficient measurements for the continuum in the frequency range where the recombination radiation appears for these levels. These measurements are discussed earlier in this paper. These data, although somewhat unprecise because the absorption is low, do not show any gross over population of these levels and certainly discount any errors larger than a factor of two in the population. A weaker argument but nevertheless a point to support the validity of the measurements for the negative-ion radiation is that when the same scheme is applied to oxygen, it was found to be quite adequate in accounting for all the oxygen continuum[6] and resulted in reasonable cross sections for the negative oxygen ion which were consistent with theoretical and also experimental values. Furthermore when this analysis was applied to argon it showed, as one would expect, no negative ion for this atom.

In considering alternative explanations for the neutral-atom recombination radiation, the only mechanisms that can be considered are those having the same temperature dependence as the nitrogen negative ion. We have made trial checks of processes such as the free-free interactions of elec-

trons with $N_2$ or $N_2^+$ species, free-bound interactions with $N_2^+$, molecular and atomic line radiation, and possibly a type of radiative association of atoms to form molecules.[35] In each case, the process either does not have the correct temperature dependence or fails to give the correct order of magnitude for the intensity.

From our data and the arguments presented we are thus left to conclude that the ($^1D$) negative ion of nitrogen is responsible for the bulk of the radiation in Fig. 13 emitted for frequencies below $1.5\times10^{15}$ sec$^{-1}$, and that the values for the experimental cross section are correct to about a factor of 2.


## ACKNOWLEDGMENTS

The authors gratefully acknowledge the encouragement and support of this work by P. Schreiber and E. Soehngen of ARL office of Aerospace Research, Wright-Patterson Air Force Base, R. Liebermann for programming the $N^+$ radiation calculations, J. Shea for his construction of the equipment used in this work.


## APPENDIX

While the calculation of the $N^+$ free-free and free-bound radiation is a straightforward matter in concept, the actual details of the calculation namely, the use of the various cross sections available, the lumping of terms, the treatment of levels for which there are no published data, the choice of the shift of the absorption edges, involve decisions which must be presented to those making comparisons of our results with other work. Toward this purpose the following Appendix gives an account of the $N^+$ continuum calculations used for the comparison of some of our data with theory.

The continuum emission intensity due to recombination and bremsstrahlung processes, in terms of power per unit volume, frequency interval, and solid angle, may be expressed as

$$I_{\mathrm{ff+fb}}(\nu)=\frac{8a^3Z^2g_f(\nu,T)kTU^+N^0}{3\sqrt{3}\pi U^0}\times\exp[-(h\nu+E_\infty{}^0-\Delta E_\infty{}^0)/kT]+\sum\frac{16a^3E_{\mathrm{H}}Z^4g_s{}^+N^0}{3\sqrt{3}\pi n^3U^0}G_{nl}{}^0\times\exp[-(h\nu+E_\infty{}^0-\Delta E_\infty{}^0)/kT]\ , \quad \text{(A1)}$$

where the first term is the Kramers free-free estimate and the second sum represents the superposition of all recombination continua for which the excitation energies, $E_{n,l}{}^0$, fulfill the condition

$$h\nu\geq E_\infty{}^0-\Delta E-E_{n,l}{}^0\geq 0.0\ , \quad \text{(A2)}$$

$n$ and $l$ being the principal and orbital quantum number, respectively, of the final state.

In the above and following expressions, $\alpha$, $h$, $a_0$, $c$, and $k$ are the usual constants; $E_{\mathrm{H}}$ is the Rydberg constant in energy units; $Z$ is the effective nuclear charge; $N^0$ is the total atom number density; $U^0$ is the internal partition function of the atom; $U^+$ is the internal partition function of the ion; $g_s{}^+$ is the ground-state statistical weight of the ion; $g_f(\nu,T)$ is the free-free Gaunt factor; $g_{\mathrm{fb}}(\nu,n)$ is the free-bound Gaunt factor; $E_\infty{}^0$ is the ionization energy of the atom while $\Delta E_\infty{}^0$ accounts for its lowering; $E_{n,l}{}^0$ is the excitation energy of the final state; $\Delta E$ is the advance of the series limit assumed equivalent to $\Delta E_\infty$; and the term $G_{n,l}{}^0$ takes into account the radiative cross sections.

For principal quantum numbers $n\geq 2$, $G_{n,l}{}^0$ is defined as

$$G_{n,l}{}^0=\sigma_{n,l}{}^0g_{n,l}{}^0/\sigma_{n,\mathrm{cl}}g_s{}^+2n^2\ , \quad \text{(A3)}$$

where $g_{n,l}{}^0$ is the degeneracy factor equal to $(2S+1)(2L+1)$ for the $n,l$ state, having a photoionization cross section $\sigma_{n,l}{}^0$. The term $\sigma_{n,\mathrm{cl}}$ represents the classical hydrogenic cross section. If hydrogenic conditions are assumed, the ratio $\sigma_{n,l}{}^0/\sigma_{n,\mathrm{cl}}$ in Eq. (A3) may be replaced by the free-bound Gaunt factor $g_{\mathrm{fb}}(n,\nu)$.

The classical hydrogenic cross section is defined as

$$\sigma_{n,\mathrm{cl}}=(64\pi\alpha a_0{}^2/3\sqrt{3})(E_{\mathrm{H}}/h\nu)^3Z^4/n^5\ . \quad \text{(A4)}$$

The free-bound Gaunt factor (approximately equivalent to 1.0 for most spectral ranges of interest) has, as was suggested by Peach,[36] been defined as

$$g_{\mathrm{fb}}=1.0+[\eta(\nu/\nu_1)^{1/3}+\beta(\nu/\nu_1)^{2/3}]-n^{-2}[\eta(\nu/\nu_1)^{-2/3}+\tfrac{2}{3}\beta(\nu/\nu_1)^{-1/3}]+n^{-4}\tfrac{2}{3}\beta(\nu/\nu_1)^{-4/3}\ , \quad \text{(A5)}$$

with

$$\eta=0.1728,\quad \beta=-0.0496,\quad \text{and}\quad \nu_1=E_{\mathrm{H}}/h\ .$$

Equation (A1) has been programmed for solution utilizing an IBM 360 computer. For ease of solution the sum term has been expanded into the following expression:

$$\sum_{n,l}=\sum_{2,l}\frac{2h\nu^3N^0}{c^2U^0}\sigma_{2,l}{}^0g_{2,l}{}^0\times\exp[-(h\nu+E_{2,l}{}^0)/kT]+\sum_{3,l}\frac{16\alpha^3E_{\mathrm{H}}Z^4g_s{}^+N^0}{3\sqrt{3}\pi n^3U^0}G_{3,l}{}^0$$

$$\times \exp[-(h\nu + E_{3,l}{}^{0})/kT]$$

$$+ \sum_{3,lp} \frac{2hN^0}{c^2U^0} \nu^3 \sigma_{3,lp}{}^{0} g_{3,lp}{}^{0}$$

$$\times \exp[-(h\nu + E_{3,lp}{}^{0})/kT]$$

$$+ \sum_{n=4}^{n_{\max}} \sum_{l}^{l_f(n)} \frac{2h\nu^3 N^0}{c^2 U^0} g_{\mathrm{fb}} R(T)$$

$$\times \sigma_{n,\mathrm{cl}} g_{n,l}{}^{0} \exp[-(h\nu + E_{n,l}{}^{0})/kT]$$

$$+ \sum_{n=4}^{n_{\max}} \frac{2h\nu^3 N^0}{c^2 U^0} g_{\mathrm{fb}} R(T) \sigma_{n,\mathrm{cl}}$$

$$\times \left( 2g_s{}^{+} n^2 - \sum_{l}^{l_f(n)} g_{n,l}{}^{0} \right)$$

$$\times \exp[-(h\nu + E_{\infty}{}^{0} - Z^2 E_{\mathrm{H}}/n^2)/kT] \,. \quad \text{(A6)}$$

In the above expression the first sum ($n=2$) contributes its continua mainly in the ultraviolet region while the second and third sums ($n=3$) contribute mostly in the visible region. The last-two sums are more prominent in the infrared region.

For the calculation of the total positive-ion radiation as a function of frequency, inputs, to Eqs. (A1) and (A6) were as follows: The determination of the bremsstrahlung contribution from the first term in Eq. (A1) was made using the free-free Gaunt factor $g_f(\nu, T)$ calculated from the tables of Karzas and Latter.[5] Inputs of the terms $\sigma_{n,l}{}^{0}$ and $G_{3,l}{}^{0}$ in terms 1 and 2 of Eq. (A6) were made available by utilizing the quantum-defect method proposed by Burgess and Seaton[4] to determine photo-ionization cross sections of species exhibiting $LS$ coupling. Such values have been calculated and published by Hahne[21] for the vacuum ultraviolet (term 1) and Griem[17] in the visible (term 2). The infrared terms, $4 \leq n \leq n_{\max}$, have been assumed hydrogenic in nature and the absorption cross section has been replaced by the classical expression, $\sigma_{n,\mathrm{cl}}$ and the free-bound gaunt factor, $g_{\mathrm{fb}}$ as defined by Peach.[36] The infrared terms are summed to an upper limit $n_{\max}$ imposed by the advance of the series limit. As suggested by Griem, $n_{\max}$ was determined by

$$n_{\max} \simeq (Z^2 E_{\mathrm{H}}/\Delta E)^{1/2} \,, \quad \text{(A7)}$$

where the advance of the series limit ($\Delta E \simeq \Delta E_{\infty}$) is given as

$$\Delta E \simeq 4E_{\mathrm{H}}[(a_0 Z)^3 N_e]^{4/15} \quad \text{(A8)}$$

with $N_e$ being the electronic number density.

Excitation energies $E_{n,l}{}^{0}$ for most of the principal quantum numbers are provided by Moore.[37] $E_{n,l}{}^{0}$ values not listed in Moore's table have been improvised. Those for $n \geq 4$ have been estimated by the hydrogenic relation.

$$E_{n,l}{}^{0} \simeq E_{\infty}{}^{0} - Z^2 E_{\mathrm{H}}/n^2 \,. \quad \text{(A9)}$$

This approximation is exhibited in the last sum term of Eq. (A6) wherein the term,

$$2g_s{}^{+} n^2 - \sum_{l}^{l_f(n)} g_{n,l}{}^{0}$$

represents the sum of the $(2S+1)(2L+1)$ degeneracy factors not listed by Moore, with the term

$$\sum_{l}^{l_f(n)} g_{n,l}{}^{0}$$

summing those that are. The resulting intensity calculated from term 6 [Eq. (A6)] was found to be of approximately the same order of magnitude as that from term 5.

In our calculation we also took into account the recombination of electrons with excited ions. Continua contributions for states where $n=3$ was accounted for by inclusion of the third sum in Eq. (A6). The subscript "$p$" denotes prime levels ($l'$) listed by Moore. Missing prime level excitation energies, $E_{3,lp}{}^{0}$ have been obtained by isoelectronic extrapolation. In calculating $\sum_{3,lp}$ sum, Eq. (2) was replaced by

$$h\nu \geq E_{\infty,p}{}^{0} - \Delta E - E_{n,lp}{}^{0} \geq 0, 0 \,, \quad \text{(A10)}$$

where the ionization level $E_{\infty,p}{}^{0}$ was approximated by

$$E_{\infty,p}{}^{0} \simeq E_{\infty}{}^{0} + E_{n,l}{}^{+} \quad \text{(A11)}$$

$E_{n,l}{}^{+}$ being the excitation energy of the excited ion in question. Hydrogenic cross sections were used for $\sigma_{3,lp}{}^{0}$ in this term.

For the hydrogenic terms ($n \geq 4$) inclusions of the factor $R(T)$ accounted for recombination of electrons with excited ions.

$$R(T) = U^{+}/g_s{}^{+} \,. \quad \text{(A12)}$$

However, the major fraction of the radiation in the red is due to the free-free process. Therefore since the recombination radiation is of less importance in this region the contribution of prime terms in the red was negligible and the factor $R(T)$ was taken as unity.

The resulting analytical intensities for the total spectral nitrogen positive ion continuum have been shown in Figs. 1, 2, 8, 9, and 10 along with the experimental data.

*The research reported herein is part of the research program on radiation from arc-heated plasma of the Aerospace Research Laboratories, Office of Aerospace Research of the U. S. Air Force, whose support is acknowledged. [Contract No. AF33 (615)-2976.]

[1]J. C. Morris, R. U. Krey, and G. R. Bach, J. Quant. Spectry. Radiative Transfer 6, 727 (1966).

[2]W. Lochte-Holtgreven, Rep. Prog. Phys. 21, 312 (1958).

[3]H. N. Olsen, Phys. Rev. 124, 1703 (1961).

[4]A. Burgess and M. J. Seaton, Monthly Notices Roy. Astron. Soc. 120, 121 (1960).

[5]W. J. Karzas and R. Latter, Astrophys. J. Suppl. Ser. 6, 167 (1961).

[6]J. C. Morris, R. U. Krey, and G. R. Bach, Phys. Rev. 159, 113 (1967).

[7]J. B. Shumaker, Rev. Sci. Instr. 32, 65 (1961).

[8]W. L. Barr. J. Opt. Soc. A., 52, 885 (1962).

[9]J. C. Morris, J. Opt. Soc. A., 51, 798 (1961).

[10]J. C. Morris and R. L. Garrison, J. Quant. Spectry. Radiative Transfer 6, 899 (1966).

[11]W. L. Wiese, M. W. Smith, and B. M. Glennon, Atomic Transition Probabilities, U. S. National Bureau of Standards National Standard Reference Data Series–4 (U. S. Government Printing Office, Washington, D. C., 1966).

[12]D. R. Bates and A. Damgaard, Phil. Trans. Roy. Soc. (London) A242, 101 (1949).

[13]C. H. Popenoe and J. B. Shumaker, Jr., J. Res. Natl. Bur. Std. A 69A, 495 (1965) (also private communication.)

[14]J. Richter, Z. Astrophys. 61, 57 (1965).

[15]H. N. Olsen, J. Quant. Spectry. Radiative Transfer 3, 59 (1963).

[16]K. W. Drellishak, D. P. Aeschliman, and Ali Bulent Cambel, Arnold Engineering Development Center, U. S. Air Force Systems Command, U. S. Air Force Technical Documentary Report No. AEDC-TDR-64-12, 1964 (unpublished).

[17]H. R. Griem, Plasma Spectroscopy (McGraw-Hill Book Co. Inc., New York, 1964).

[18]G. Boldt, Z. Physik 154, 330 (1959).

[19]G. M. Thomas and W. A. Menard, Am. Inst. Aeron. Astron. 5, 2214 (1967).

[20]H. A. Kramer, Phil. Mag. 46, 836 (1923).

[21]G. E. Hahne, National Aeronautics and Space Administration Report No. NASA TN D-2794, 1965 (unpublished).

[22]R. A. Allen and A. Textoris, J. Chem. Phys. 40, 3445 (1964).

[23]G. E. Norman, Opt. i Spektroskopiya 17, 176 (1964) [English transl.: Opt. Spectry. 17, 94 (1964)].

[24]R. Taylor, to be published in J. Quant. Spectry. Radiative Transfer.

[25]Yu. V. Moskvin, Opt. i Spektroskopiya 17, 499 (1964) [English transl.: Opt. Spectry. 17, 270 (1964)].

[26]B. Edlen, J. Chem. Phys. 33, 98 (1960).

[27]G. Glockler, J. Chem. Phys. 32, 708 (1960).

[28]C. W. Scherr, J. N. Silverman, and F. A. Matsen, Phys. Rev. 127, 830 (1962).

[29]H. R. Johnson and F. Rohrlich, J. Chem. Phys. 30, 1608 (1958).

[30]J. W. Edie and F. Rohrlich, J. Chem. Phys. 36, 623 (1962).

[31]A. P. Ginsberg and J. M. Miller, J. Inorg. Nucl. Chem. 7, 351 (1958).

[32]Ya. M. Fogel, V. F. Kozlov, and A. A. Kalmykov, Zh. Eksperim. i Teor. Fiz. 36, 1354 (1959) [English transl.: Soviet Phys. – JETP 9, 963 (1960)].

[32a]E. I. Asinovskiy, A. V. Kivillin, and G. A. Kobzev, Teplofizika Vysokikh Temperatur, No. 4, 746, Moscow, (1968).

[33]S. Chandrasekhar and M. K. Krogdahl, Astrophys. J. 98, 205 (1943).

[34]A. Dalgarno and A. E. Kingston, Proc. Phys. Soc. (London) 73, 455 (1959).

[35]D. R. Bates, Monthly Notices Roy. Astron. Soc. 111, 303 (1951).

[36]G. Peach, Monthly Notices Roy. Astron. Soc. 124, 372 (1962).

[37]C. E. Moore, Atomic Energy Levels, National Bureau of Standards Circular No. 467 (U. S. Government Printing Office, Washington, D. C. 1949), Vol. I.